A novel unspecific peroxygenase from Agaricus bisporus var. bisporus for biocatalytic oxyfunctionalisation reactions

Li, Tiantian; Liang, Hongjing; Wu, Bin; Lan, Dongming; Ma, Yunjian; Hollmann, Frank; Wang, Yonghua

DOI
10.1016/j.mcat.2023.113275

Publication date
2023

Document Version
Final published version

Published in
Molecular Catalysis

Molecular Catalysis 546 (2023) 113275

Contents lists available at ScienceDirect

Molecular Catalysis

journal homepage: www.journals.elsevier.com/molecular-catalysis

A novel unspecific peroxygenase from *Agaricus bisporus* var. *bisporus* for biocatalytic oxyfunctionalisation reactions

Tiantian Li [a], Hongjing Liang [b], Bin Wu [b], Dongming Lan [a], Yunjian Ma [a,*], Frank Hollmann [c,*], Yonghua Wang [a,d,**]

[a] School of Food Science and Engineering, South China University of Technology, Guangzhou 510640, China
[b] School of Bioscience and Bioengineering, South China University of Technology, Guangzhou 510006, China
[c] Department of Biotechnology, Delft University of Technology, van der Maasweg 9 2629 HZ, Delft, The Netherlands
[d] Guangdong Youmei Institute of Intelligent Bio-manufacturing Co., Ltd, Foshan, Guangdong 528200, China

ARTICLE INFO

Keywords:
Unspecific peroxygenase
Agaricus bisporus var. bisporus
Heterologous expression
Heme-thiolate peroxidase
Oxyfunctionalisation

ABSTRACT

Unspecific peroxygenases (UPOs) represent an emerging class of catalysts for the selective oxyfunctionalisation of C—H- and C = C groups. Until now, only a few UPOs have been characterised. In this study, we report a new peroxygenase identified from the Unspecific Peroxygenase Database. The UPO from *Agaricus bisporus* var. *bisporus* (*Abvb*UPO) has been heterologously expressed in *Aspergillus niger* and initially characterised with respect to its basic biochemical features. Furthermore, its catalytic properties were evaluated with enzymatic cascade reactions of choline oxidase (*AnChOx*) and *Abvb*UPO, which the *AnChOx* provided H_2O_2 necessary via reductive activation of oxygen *in situ*. Three types of oxyfunctionalizations, such as hydroxylation of ethylbenzene, epoxidations of styrene and cyclohexene, sulfoxidations of methyl phenyl sulfide and phenyl vinyl sulfide, were successfully achieved. We also investigated the activity of *Abvb*UPO on fatty acids in some more detail. The experimental results show that Under the above conditions, *Abvb*UPO had the higher activity for cyclohexene epoxidation and sulfonation of sulfide substrates. The concentration of epoxy cyclohexane was 2.91 mM, and the concentration of methyl phenyl sulfoxide was 3.69 mM. The regioselectivity of *Abvb*UPO was ω-1 bonds position of linear saturated fatty acid. All in all, *Abvb*UPO exhibits some interesting differences which may put the basis for further understanding of the factors determining peroxygenase selectivity.

1. Introduction

Unspecific peroxygenases (UPOs, EC 1.11.2.1) are very promising alternatives to the existing chemical and enzymatic catalysts for specific oxyfunctionalisation reactions [1–4]. Compared to the currently favoured P450 monooxygenases, UPOs excel by their much simpler molecular architecture relying on H_2O_2 only instead of complex electron transport chains [5–8]. At the same time, UPOs give access to the same types of oxyfunctionalisation (such as hydroxylation and epoxidation) reactions as P450 monooxygenases [9,10]. Issues related to the oxidative inactivation of the catalytic heme prosthetic group can be considered as solved as today a range of H_2O_2 generation systems are available enabling to maintain the *in situ* H_2O_2 concentration low enough to minimise inactivation but sufficiently high to attain high reaction rates [11].

Today, however, only a handful of UPO (variants) are known and consequently, the product scope is still rather limited. Next to the archetypal UPO from *Agrocybe aegerita* (*Aae*UPO) [12–21], UPOs from *Coprinellus radians* (*Cra*UPO) [14,15], *Coprinopsis cinerea* (*Cci*UPO) [19–24], *Marasmius rotula* (*Mro*UPO) [18–21,24,25–29], *Chaetomium globosum* (*Cgl*UPO) [21,24,29–31], *Collariella virescens* (*Cvi*UPO) [32], *Humicola insolens* (*Hin*UPO) [21,31], *Hypoxylon* sp. *EC38* (*Hsp*UPO) [33] and *Myceliophthora thermophila* (*Mth*UPO) [34] have been reported exhibiting interesting differences in their substrate scope and selectivities. Nevertheless, the need for a broader basis of UPOs remains. In previous works we have set up an Unspecific Peroxygenase Database (UPObase) identifying new putative UPO sequences from fungal genomes. As a guiding principle, we used the conserved PCP motif for the distal cysteine ligand and the EGD-S-R-E (EHD-S-E) motif screen for new peroxygenases. In total 1948 putative UPO-encoding sequences had

* Corresponding authors.
** Corresponding author at: School of Food Science and Engineering, South China University of Technology, Guangzhou 510640, China.
E-mail addresses: femayj@mail.scut.edu.cn (Y. Ma), f.hollmann@tudelft.nl (F. Hollmann), yonghw@scut.edu.cn (Y. Wang).

https://doi.org/10.1016/j.mcat.2023.113275
Received 5 March 2023; Received in revised form 4 May 2023; Accepted 24 May 2023
Available online 30 May 2023

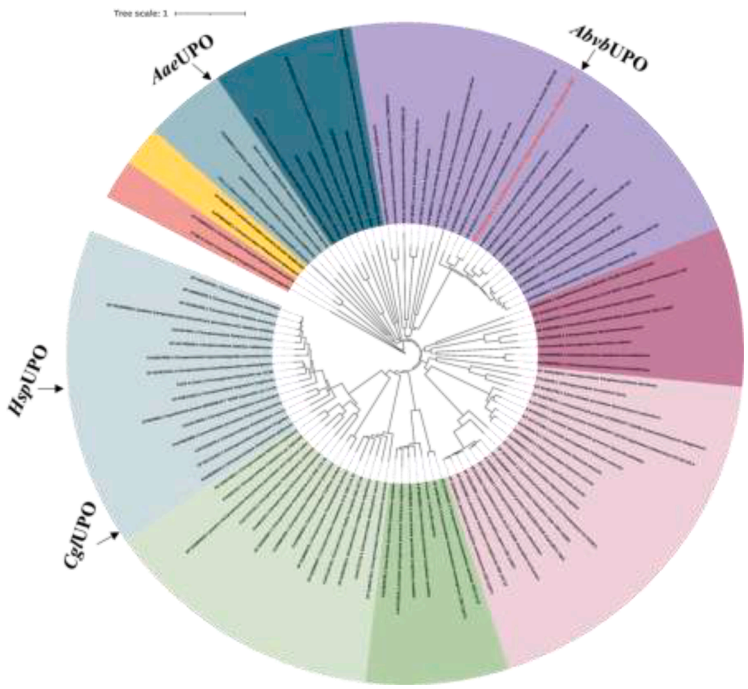

Fig. 1. Phylogenetic tree analysis of UPO genes and localization of *Abvb*UPO. For a full overview including sequences and accession numbers refer to the SI.

been identified [35].

In this work, we report on the identification, expression, and initial characterisation of a novel peroxygenase from *Agaricus bisporus* var. *bisporus* (*Abvb*UPO). The phylogenetic analysis of *Abvb*UPO showed that *Abvb*UPO was not clustered together with *Aae*UPO, *Hsp*UPO or *Cgl*UPO in the phylogenetic tree (Fig. 1). Hence, *Abvb*UPO may exhibit some interesting structural and catalytic differences compared to the 'gold standard' peroxygenase *Aae*UPO.

2. Materials and methods

2.1. Cells, plasmid, and chemicals

Escherichia coli (*E. coli*) DH5α competent cells were purchased from Weidi Biotechnology Co., Ltd (Shanghai, China) and the *Aspergillus niger* strain ATCC 1015 was purchased from Guangdong Provincial Microbial Culture Preservation centre (Guangzhou, China). The pBC—Hygro vector was purchased from Thermo Fisher Technology Co., Ltd (Shanghai, China). All chemicals were purchased from TCI (Shanghai, China) Development Co., Ltd., Shanghai Aladdin Biochemical Technology Co., Ltd., or Sigma-Aldrich (Shanghai, China) in the highest purity available and used without further treatment.

2.2. Amino acid sequence analysis of AbvbUPO

The FASTA sequence of *Abvb*UPO (XP_006457061.1) was obtained from NCBI (https://www.ncbi.nih.gov.in) and refined for sequence consistency alignment using DNAMAN (http://multalin.toulouse.inra.fr/multalin). The sequence homology of *Abvb*UPO was compared with other "long" UPOs (*Aae*UPO, *Gma*UPO, *Hsu*UPO, *Man*UPO, *Col*UPO, *Ame*UPO, *Ran*UPO, and *Ana*UPO) (Fig. S1) and was analysed by ESPript 3.0 [36] (http://espript.ibcp.fr/ESPript/cgi-bin/ESPript.cgi).

2.3. Homology modelling of AbvbUPO

To build the homology model for *Abvb*UPO we used Swiss-Model (http://swissmodel.expasy.org/) for template recognition and selected the template exhibiting the highest homology. heme was manually added to the apoenzyme using PyMOL.

2.4. Construction of plasmid

The nucleotide sequence of the *Abvb*UPO gene (XP_006457061.1) and phytase signal peptide were purchased as codon-optimised (for *A. niger*) sequences from Shanghai Sangon Biotechnology (Shanghai, China). We added a phytase signal peptide to the N-terminal (to promote the extracellular secretion of target protein). For purification, a 6×His-tag was added to the C-terminal. The fragments of promoter PglaA (glucoamylase promoter), TglaA (glucoamylase terminator), phytase signal peptide and *Abvb*UPO were amplified using the specific primers (Table S1). PCR reactions were performed using a thermocycler (Bio-Rad, Hercules, CA) in a final volume of 50 μL containing 10 μM of each primer, 50 ng template, and 25 μL Primer Star Max (Takara, Dalian, China). The running program was set as 98℃ for 5 min (1 cycle); 98 ℃ for 15 s, 55 ℃ for 15 s, 72 ℃ for 1.5 min (30 cycles), and 72℃ for 5 min (1 cycle). The PCR product and the linearised pBC vector were purified with the Gel DNA Recovery kit (Shanghai Sangon Biotechnology, Shanghai, China). The target gene, promoter, and pBC linearisation vector were linked using the T4 DNA ligase kit (Thermo Scientific, Shanghai, China) followed by heat shock transformation into chemically competent *E. coli* DH5α cells. After sequencing verification, the correct recombinant expression vector was named pBC-PglaA-*Abvb*UPO-glaT (Fig. S2).

2.5. Transformation and expression

Aspergillus niger strain ATCC 1015 was cultured in DPY medium containing 2% (*w/v*) glucose, 1% (*w/v*) peptone, 0.5% (*w/v*) yeast extract, 0.5% (*w/v*) KH_2PO_4, 0.05% (*w/v*) $MgSO_4 \bullet 7H_2O$. The verified recombinant plasmid pBC-PglaA-*Abvb*UPO-glaT was linearised by HindIII restriction endonuclease and integrated into the genome of *A. niger* by homologous recombination using the protoplast transformation method: *Aspergillus niger* strains were ground and cracked, and the lysate was filtered and centrifuged to obtain precipitated protoplasts. After washing with precooled 0.6 M KCl, the protoplast weight was suspended in Scarlett C solution (1 M sorbitol, 50 mM $CaCl_2$) followed by gentle

mixing with the linearised plasmid. 50 μL PEG solution was added, and 1 mL PEG buffer was slowly added in ice bath for 30 min. After 20 min at 25 ℃, the protoplast weight was mixed and coated on PDA plate (containing 200 μg/mL Hyg B). It was cultured at 34 ℃ for 5–6 days and the positive transformants were screened on MM plates (2% (*w/v*) glucose, 0.3% (*w/v*) $NaNO_3$, 0.1% (*w/v*) KH_2PO_4, 0.2% (*w/v*) KCl, 0.05% (*w/v*) $MgSO_4•7H_2O$, and 0.001% (*w/v*) $FeSO_4•7H_2O$, pH 5.5), identified by PCR reactions and verified by DNA sequencing.

Confirmed transformants were inoculated into 100 mL CD culture medium (3% (*w/v*) sucrose, 0.2% (*w/v*) $NaNO_3$, 0.1%(*w/v*) KH_2PO_4, 0.05%(*w/v*) $MgSO_4$, 0.05%(*w/v*) KCl, 0.001% (*w/v*) $FeSO_4•7H_2O$, 0.05% (*w/v*) agar) with conditions of incubating in the incubator at 30–32℃ for 2 days. Then, the spore suspension was transferred to the Potato Dextrose Broth medium (3.5% (*w/v*) potato, 0.35% (*w/v*) dextrose)with 5% of the inoculation amount, with a shaking speed at 220 rpm for 48 h at 30 ℃ in 500 mL flask. Subsequently, the seed solution was inoculated into a 5 L bioreactor with an inoculation amount of 10% (*v/v*). The whole fermentation process was run at 30℃ and 800 rpm, with a ventilation volume of 7 vvm, and the pH was maintained at 5.0. After 15 h of fermentation, a 50% glucose solution was added for feeding. Cultures were sampled at 12 h intervals over 7 days, the changes of cell wet weight and OD_{600} in culture medium were recorded, and extracellular *Abvb*UPO activities were determined after the harvested supernatants were centrifuged and filtered. The extracellular proteins were further analysed by SDS-PAGE.

2.6. Optimisation of medium and fermentation time in high cell-density fermentation

To obtain *Abvb*UPO with higher enzyme activity, three fermentation media (CMI, CMII, CMIII) were selected to optimise the high-density fermentation of *Abvb*UPO (as shown in Table S2). Using the optimal CMII medium fermentation conditions, three fermentation times were selected to optimise the expression of *Abvb*UPO (144 h, 156 h, 168 h), other high cell-density fermentation process was conducted by the method mentioned in 2.5. Three parallels for each group of data, regarding the highest value group as 100% relative activity.

2.7. Purification of AbvbUPO

To purify the recombinant *Abvb*UPO, the culture media were collected by centrifugation (6000 rpm, 4 ℃, for 20 min) and submitted to a Nickel ion affinity chromatography column (Bergeron (Shanghai) Biotechnology Co., Ltd), which was previously equilibrated with 20 mM potassium phosphate buffer (pH 7.5), containing 20 mM imidazole. *Abvb*UPO was eluted with a gradient of 20 mM potassium phosphate buffer (pH 7.5) containing 0.5 M imidazole. Fractions containing enzyme activity were pooled. Using a gel column the buffer was changed to 50 mM Tris–HCl (pH 7.0). Fractions were pooled and enzymes were concentrated with Amicon 1 K (Millipore) until an appropriate volume. The protein content was determined by using the Bio-Rad protein assay reagent kit (Bio-Rad, Hercules, CA, USA) and bovine serum albumin as a standard. The purity of the recombinant *Abvb*UPO was checked by 10% SDS–PAGE.

2.8. Determination of abvbupo activity

For this, we used the classical peroxidase assay based on ABTS oxidation (detecting single electron abstraction activity) and the so-called NBD assay (classical peroxygenase) to detect oxy-functionalisation activity (Fig. S3). ABTS and NBD methods were shown in Table S3. One unit (U) of activity was defined as the amount of enzyme that oxidizes substrate to 1μmol of product per minute under the specified conditions [37].

2.9. Effects of temperature, pH, metal ions, organic solvents, and surfactants on purified recombinant AbvbUPO activity

The optimum temperature of the enzyme was evaluated by measuring the *Abvb*UPO activity at different temperatures (15–60 ℃) in 100 mM Tris–HCl buffer (pH 7.0) with NBD as the substrate by (2.8) method. The effect of temperature on *Abvb*UPO stability was also determined by incubating an aliquot of the enzyme in 100 mM Tris–HCl (pH 7.0) at different temperatures (30–60 ℃). The enzyme was then assayed for the remaining activity at 60 min intervals until 12 h of incubation.

The optimum pH of the enzyme was measured using NBD as the substrate. The following buffers (100 mM) were used: citrate phosphate (pH 3.0–5.0), NaH_2PO_4–Na_2HPO_4 buffer (6.0–7.0), Tris–HCl (pH 8.0–9.0), and $NaHCO_3$–NaOH (pH 10.0–11.0). The pH stability was determined by incubating *Abvb*UPO in 100 mM different buffers, (pH 3.0–11.0), for 3 h at 4℃, and its residual activity was determined at its optimal temperature and pH.

Influences of different organic solvents and surfactants on enzyme activity were evaluated. UPO activity was measured in the presence of organic solvents (methanol, ethanol, isopropyl alcohol, acetone, acetonitrile, ethyl acetate) and surfactants (SDS, Tween 20, Tween 60, Tween 80, Triton X-100) at 5 mM and 10% (v/v) concentration under optimal conditions, respectively. The NBD activity of purified *Abvb*UPO without any reagent treatment was taken as control using the above method standard assay.

2.10. Effects of H_2O_2 on recombinant AbvbUPO activity

To examine the effect of H_2O_2 concentration on *Abvb*UPO activity, the NBD assay (2.8) was performed at different H_2O_2 concentrations (1, 2, 4, 5, 8, 10, and 20 mM, respectively). The H_2O_2 tolerance of *Abvb*UPO was assessed by incubating the enzyme solution at different H_2O_2 concentrations. Samples were collected after 0, 10, 30, 60, 120, and 150 min and complemented with NBD. OD_{425} (absorbance in 425 nm) value of samples was measured in the NBD system every 30 s by a kinetic method. The difference value of OD_{425} was compared in the same linear region (5–10 min). Difference values were characterised as the relative activity of *Abvb*UPO, regarding the highest difference value group as 100% relative activity.

2.11. Catalytic reactions of AbvbUPO

Catalytic transformations involving *Abvb*UPO were performed using a previously reported *in situ* H_2O_2 generation system based on the aerobic oxidation of choline using the Choline oxidase from *Arthrobacter nicotianae* (*AnChOx*) [4]. Reactions were performed at a 1 mL scale in sealed glass vials (4 mL volume) for 24 h at 30 °C while shaking at 500 rpm. The reaction mixture (buffer: 50 mM NaPi, pH 7) contained 0.73 $mg·mL^{-1}$ *Abvb*UPO, *AnChOx* (5 μM), Choline chloride (100 mM), and substrate (25 mM aromatic substrate and 1 mM fatty acids in case of all other starting materials). The reactions were halted by adding 100 μL of HCl (0.3 M) and incubating for 5 min at 500 rpm and room temperature. Fatty acids and their derivatives were extracted with methyl tert-butyl ether (MTBE, 1 mL) and dried under Na_2SO_4. TMS-derivatisation was achieved by treatment with N, O-bis (trimethylsilyl) trifluoroacetamide (BSTFA), other compounds were extracted with ethyl acetate (1 mL), dried over Na_2SO_4, analysed on chiral GC and GC–MS, respectively. In case of chiral products, racemic standards and enentiomerically pure enantiomers were used to determine the retention times and to create calibration curves.

2.12. Gas chromatography and temperature profiles

The GC-FID analysis was performed on an Agilent 7890B GC system (Agilent Technologies, Palo Alto, CA, USA) outfitted with a J&W CP

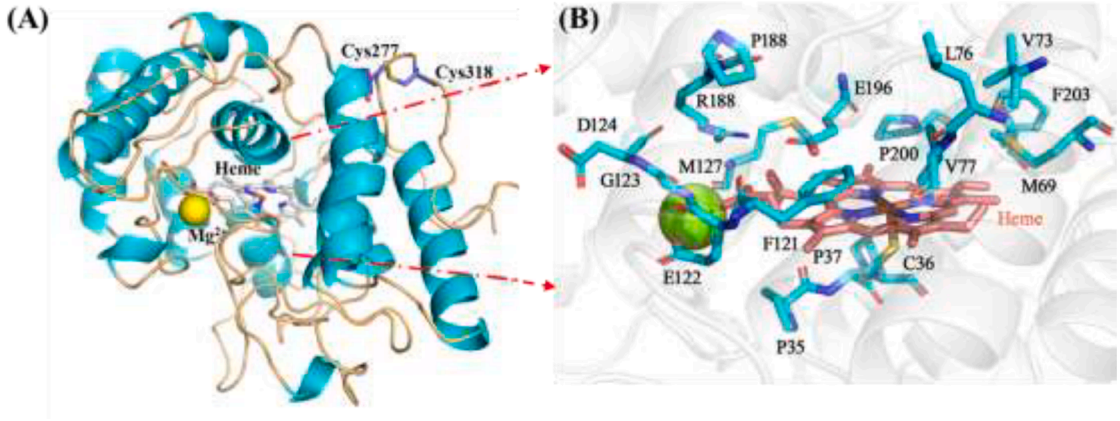

Fig. 2. *Abvb*UPO homology modelling. (A): Cartoon model of *Abvb*UPO; (B): The active site with some catalytic relevant residues around heme.

Chirasil-Dex CB column (25 m length × 0.32 mm I.D. × 0.25 μm film thickness), and an FID detector. Injection volume: 1 μL; injection temperature: 250 °C; split ratio: (30:1); detector temperature: 280 °C. For most reagents temperature program A was used except for cyclohexene (and reaction products) for whom temperature program B was used. Fatty acid (derivates were analysed via GCMS (*2.13*).

Method A: The oven was heated from 50 °C to 130 °C (1 min hold) by 10 °C /min, 3 °C/min to 150 °C (1 min hold), 25 °C/min to 200 °C (10 min hold);

Method B: The oven was heated from 50 °C to 130 °C (2 min hold) by 5 °C /min, 25 °C/min to 200 °C (10 min hold). Using standard curves, measurements were obtained from peak areas.

2.13. Gas chromatograph-mass spectrometry and temperature profiles

Fatty acid and product GC–MS analyses were performed on a Shimadzu TQ8050 Ultra (Shimadzu Technologies, Japan) equipped with Shimazu SH-Rxi-5Sil MS columns (30 m length × 0.25 mm I.D. × 0.25 μm film thickness), using He as carrier gas at a rate of 0.8 mL/min. split ratio (100:1), ion source temperature: 230 °C, solvent delay time: 3 min. The oven was heated from 50 °C (2 min hold) to 250 °C (12 min hold) at a rate of 20 °C /min for a total of 24 min. Total-ion peak areas were quantified using external standard curves and molar response factors of the same or similar compounds.

3. Results and discussion

3.1. Homologous modeling of AbvbUPO

Using the structure of *Aae*UPO (2YOR) as a template (sequence homology of 61.4%, Table S4) we constructed a homology model for *Abvb*UPO (Fig. 2). As structural elements, this homology model suggested 11 α-helices and 5 β-strands in the secondary structure of the protein (*α*1-*β*1-*α*2-*α*3-*β*2-*α*4-*α*5-*β*3-*α*6-*α*7- *β*6-*α*8-*β*4-*β*5-*α*9-*β*7-*α*10-*α*11). Pro35-Cys36-Pro37 coordinating the heme-Fe-ion are located in α1 before the helix. Glu122-Gly123-Asp124 is located in β2 and the catalytic acid-base pair Arg189-Glu196 is located in α6. A putative disulfide bridge between Cys277 and Cys318 may be involved in the stabilisation of the α9 helix and the C-terminal region. A tightly coordinated Mg^{2+} (Glu122, Gly123, Ser126) is possibly relevant for the stabilisation of the overall structure [38].

3.2. Production and purification of AbvbUPO

After initial, unsuccessful attempts to recombinantly express *Abvb*UPO in *E. coli* (formation of bacterial inclusion bodies), we focused on *Aspergillus niger* as an expression strain. The codon-optimised synthetic gene (XP_006457061.1) was subcloned into the pBC-hygro expression vector and expressed in *Aspergillus niger* strain ATCC 1015. After

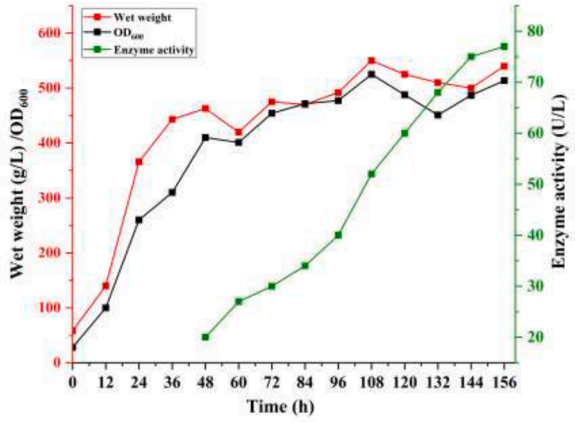

Fig. 3. Time course of the 5L-scale fermentation of *Aspergillus niger* recombinantly expressing *Abvb*UPO. Note that NBD-activity was not detectable until *t* = 48 h.

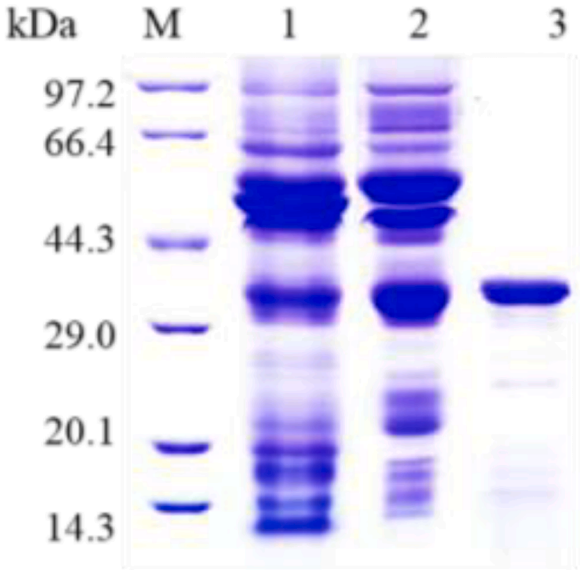

Fig. 4. SDS-PAGE analysis of expression and purification of *Abvb*UPO in *Aspergillus niger* ATCC 1015. M: Marker; Lane1-Cell lysis supernatant; Lane 2-column flow through; Lane 3–500 mM imidazole elution.

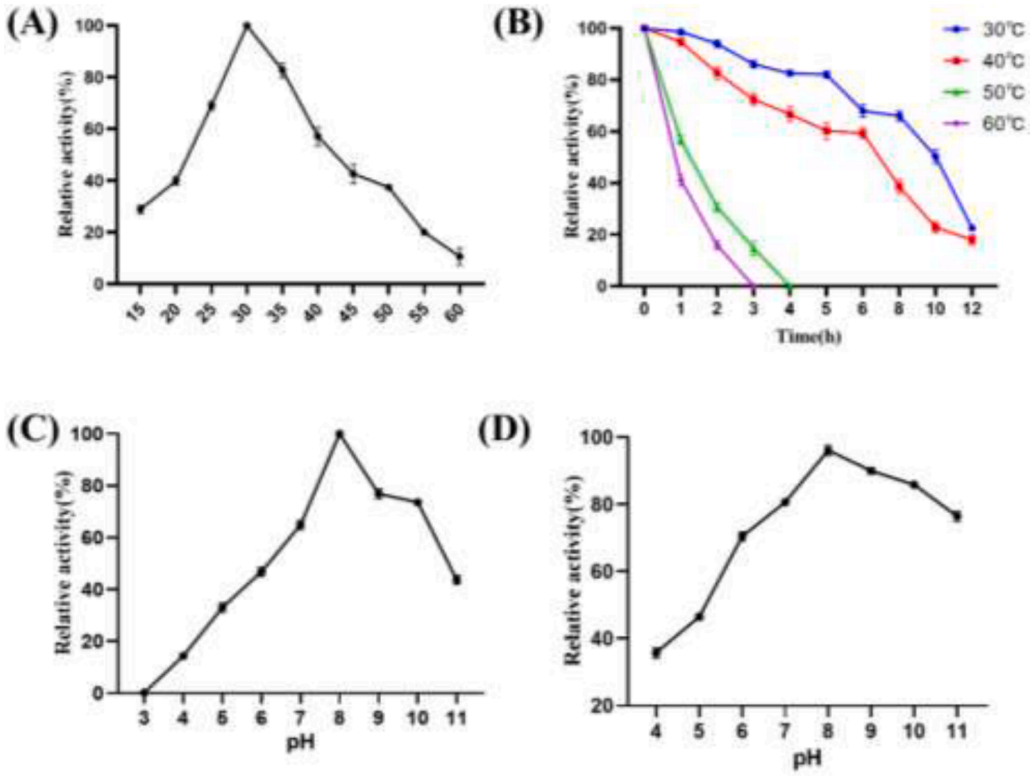

Fig. 5. The effect of temperature and pH on enzymatic properties of recombinant *Abvb*UPO.

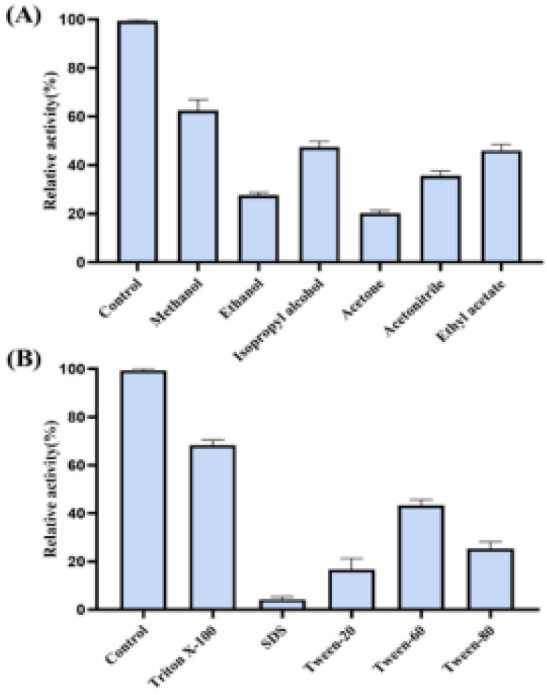

Fig. 6. Effects of organic solvents(A) and surfactants(B) on enzyme activity of *Abvb*UPO.

optimising the fermentation medium and fermentation time (Fig. S4) a 5L-scale fermentation yielded a cell wet mass of 540 g/L and an *Abvb*UPO activity of 77 U/L in the supernatant were obtained from a 5 L fermentation broth (Fig. 3).

Since the recombinant *Abvb*UPO contained a C-terminal polyhistidine tag, it was purified to near homogeneity via Ni^{2+}-affinity chromatography (Fig. 4). SDS-PAGE examination indicated the molecular mass of *Abvb*UPO to be approximately 38 kDa (Fig. 4), which is somewhat larger than the theoretical mass a molecular weight (35 kDa) and is most likely owing to glycosylation of the polypeptide chains.

3.3. Characterisation of the recombinant AbvbUPO

Having pure *Abvb*UPO at hand, we further explored some factors influencing its activity and stability. Using the NBD-assay (12 h reaction time), the enzyme activity increased up to a temperature of 30 ℃ (Fig. 5A) and steadily decreased upon further increasing the temperature. This is in line with the thermal stability of *Abvb*UPO showing a half life time of approx. 11 h at 30 °C, which considerably decreased to less than one hour at 60 ℃ (Fig. 5B). pH 8 appeared optimal for *Abvb*UPO both, for its catalytic activity (Fig. 5C) as well as for its stability (Fig. 5D). The pH spectrum was comparably broad with more than 50% of its maximal activity and stability between pH 6 and 11.

(A) Optimum temperature. (B) Thermal stability of *Abvb*UPO. (C) Optimum pH at varying pHs (pH 3.0–11.0); (D) pH stability in 100 mM varying pHs buffer for 3 h at 4 ℃).

Envisioning the transformation of hydrophobic, poorly water-soluble reactants, we also investigated the influence of several, water soluble organic solvents on the activity of *Abvb*UPO (Fig. 6). In the presence of approximately 10% (v/v) methanol, isopropanol and ethyl acetate the catalytic activity of *Abvb*UPO was lowered by less than 50% at 4℃ for 2 h. Other solvents such as methanol, acetone, or acetonitrile had a more detrimental effect on *Abvb*UPO activity. Envisioning future applications of *Abvb*UPO in biphasic reaction media comprising a hydrophobic organic phase (as substrate reservoir and product sink) we also evaluated the influence of some surfactants to be used as emulsifiers (Fig. 6B). Again, the presence of surfactants generally decreased the activity of the biocatalyst.

As a heme-dependent enzyme, *Abvb*UPO is prone to H_2O_2-induced oxidative inactivation [11]. We therefore tested the activity and robustness of *Abvb*UPO in the presence of different concentrations of

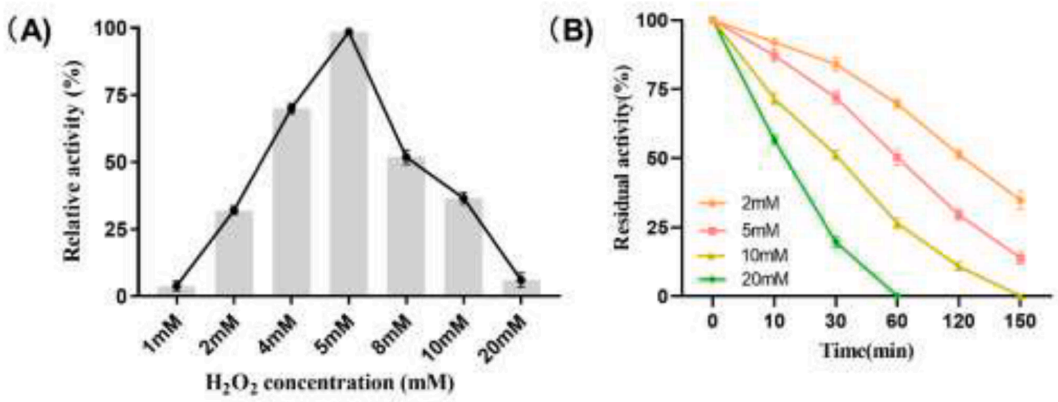

Fig. 7. The effect of H_2O_2 concentration on enzyme activity of *Abvb*UPO. (A) Optimum H_2O_2 concentration. (B) H_2O_2 stability of *Abvb*UPO.

Table 1
The preliminary substrate scope of *Abvb*UPO.

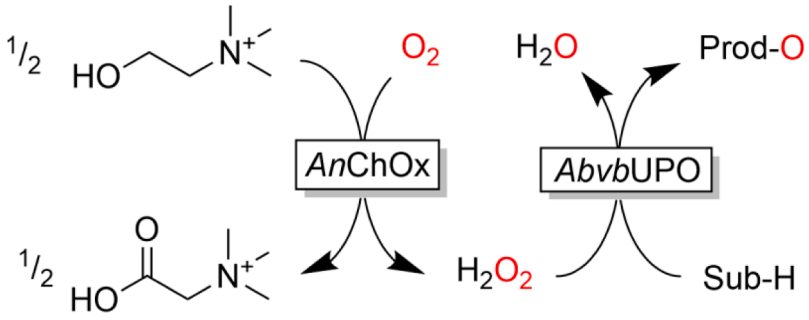

Substrate	Product		Concentration [mM]	Optical purity [%]
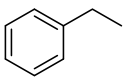	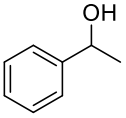		0.5	34 (R)
	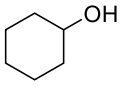		1.3	n.a.
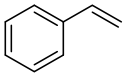	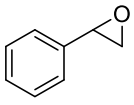		0.8	51 (S)
	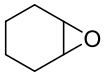		2.9	n.a.
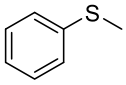	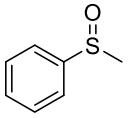		3.7	77 (R)
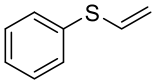	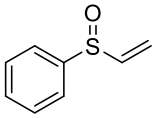		0.5	51 (R)
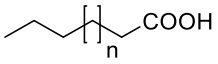	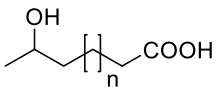	*n* =		n.d.
		3	0.02	
		4	0.09	
		5	0.16	
		6	0.30	
		7	0.23	

General conditions: [*An*ChOx] = 5 μM, [ChCl] = 100 mM, [*Abvb*UPO crude enzyme] = 0.73 mg·mL^{-1}, [Aromatic substrates] = 25 mM in NaPi buffer (pH 7.0, 50 mM) system, 500 rpm, 24 h, 30 °C.
[Saturated fatty acid substrates] = 1 mM in NaPi buffer (pH 7.0, 50 mM) system, 500 rpm, 12 h, 30 °C.

H_2O_2 (Fig. 7). *Abvb*UPO activity almost linearly increased up to an H_2O_2 concentration of 5 mM indicating the *Abvb*UPO affinity towards H_2O_2 may not be very high (with a K_M value of at least 2.5 mM). Increasing the *in situ* concentration of H_2O_2 is not advisable as the inactivation rate of *Abvb*UPO is directly correlated with the H_2O_2 concentration applied (Fig. 7B).

3.4. Substrate scope of AbvbUPO

The quantitative determination and enantiomeric excess determination of the product is determined by GC, and the identification and analysis of the product were determined by GC–MS. See SI for the detailed chromatogram and gas chromatograph (Figs. S5–S16).

To preliminarily evaluate the substrate scope of *Abvb*UPO we tested a range of commonly used starting materials (Table 1). To minimise the oxidative inactivation of the peroxygenases, we relied on a recently established *in situ* H_2O_2 generation system based on the choline oxidase (from *Arthrobacter nicotianae, An*ChOx) catalysed oxidation of choline to betaine (Table 1) [39–41].

Interestingly, ethyl benzene was hardly converted by *Abvb*UPO. Furthermore, the enantioselectivity was very low. In contrast, the less activated cyclohexane gave comparably high conversion. Even more interestingly, in case of cyclohexene only the epoxidation product was observed. This is interesting insofar as today UPO-catalysed epoxidations are generally plagued by the competing allylic hydroxylation reaction resulting in complex product mixtures. The seemingly high epoxidation selectivity will certainly be investigated in more depth in future studies.

Also in case of phenyl vinyl sulphide some interesting new product peaks were detected (Fig. S10) which using *Aae*UPO had not been detected [40]. Currently, we are lacking a plausible mechanistic explanation for the formation of the putative coupling products and further spectroscopic and kinetic studies will be necessary to fully understand the formation of these side-products.

A range of medium-chain fatty acids were converted by *Abvb*UPO. In Table 1, the concentrations of the ω−1-hydroxy products are shown. It should, however be mentioned that the fatty acid hydroxylations were not very regioselective as judged by the complex GC traces (Figs. S11–15). This indicates a higher active site plasticity as compared to wt-*Aae*UPO [42] and may put the basis for the semi-rational design of UPO variants with tailored fatty acid hydroxylation selectivity.

4. Conclusion

In this study, we report a novel peroxygenase from *Agaricus bisporus* var. *bisporus* (*Abvb*UPO) enriching the peroxygenase toolbox. In its basic features, *Abvb*UPO resembles the UPOs known so far. However, it also exhibits a range of interesting differences in substrate scope and product selectivity. Further investigations on the substrate scope and selectivity of *Abvb*UPO will enable a molecular understanding of the selectivity differences and will open up new avenues for designing tailored peroxygenases.

CRediT authorship contribution statement

Tiantian Li: Conceptualization, Investigation, Visualization, Validation. **Hongjing Liang:** Conceptualization, Investigation, Visualization, Validation. **Bin Wu:** Formal analysis, Investigation, Validation. **Dongming Lan:** Project administration, Investigation, Validation. **Yunjian Ma:** Formal analysis, Investigation, Validation. **Frank Hollmann:** Data curation, Writing – original draft, Project administration, Investigation, Validation. **Yonghua Wang:** Project administration, Investigation, Validation.

Declaration of Competing Interest

The authors declare that they have no known competing financial interests or personal relationships that could have appeared to influence the work reported in this paper.

Data availability

Data will be made available on request.

Acknowledgments

This work was supported by the National Natural Science Foundation of China (32001633), Guangzhou Science and technology planning project (202102020370), the Key Program of Natural Science Foundation of China (31930084).

Supplementary materials

Supplementary material associated with this article can be found, in the online version, at doi:10.1016/j.mcat.2023.113275.

References

[1] R. Ullrich, M. Hofrichter, Oxidations catalyzed by fungal peroxygenases, Curr. Opin. Chem. Biol. 19 (2014) 116–125.
[2] Y.H. Wang, D.M. Lan, R. Durrani, F. Hollmann, Peroxygenases en route to becoming dream catalysts. What are the opportunities and challenges? Curr. Opin. Chem. Biol. 37 (2017) 1–9.
[3] R. Ullrich, A. Karich, M. Hofrichter, Fungal Peroxygenases – A Versatile Tool for Biocatalysis, Encycl. Mycol. 2 (2021) 260–280.
[4] M. Hobisch, D. Holtmann, P.G.D. Santos, M. Alcalde, F. Hollmann, S. Kara, Recent developments in the use of peroxygenases–Exploring their high potential in selective oxyfunctionalisations, Biotechnol. Adv. 51 (2021) 107615–107628.
[5] S. Bormann, A.G. Baraibar, Y. Ni, D. Holtmann, F. Hollmann, Specific oxyfunctionalisations catalysed by peroxygenases: opportunities, challenges and solutions, Catal. Sci. Technol. 5 (2015) 2038–2052.
[6] M. Hofrichter, H. Kellner, M.J. Pecyna, R. Ullrich, Fungal unspecific peroxygenases: heme-thiolate proteins that combine peroxidase and cytochrome P450 properties, Adv. Exp. Med. Biol. 851 (2015) 341–368.
[7] M. Faiza, S.F. Huang, D.M. Lan, Y.H. Wang, New insights on unspecific peroxygenases: superfamily reclassification and evolution, BMC Evol. Biol. 19 (2019) 76–95.
[8] A. Kinner, K. Rosenthal, S. Lütz, Identification and expression of new unspecific peroxygenases–recent advances, challenges and opportunities, Front. Bioeng. Biotechnol. 9 (2021) 704630–705647.
[9] Y.F. Wei, E.L. Ang, H.M. Zhao, Recent developments in the application of P450 based Biocatalysts, Curr. Opin. Chem. Biol. 43 (2018) 1–7.
[10] V.B. Urlacher, M. Girhard, Cytochrome P450 monooxygenases in biotechnology and synthetic biology, Trends Biotechnol. 37 (2019) 882–897.
[11] B.O. Burek, S. Bormann, F. Hollmann, J.Z. Bloh, D. Holtmann, Hydrogen peroxide driven biocatalysis, Green Chem. 21 (2019) 3232–3249.
[12] R. Ullrich, J. Nüske, K. Scheibner, J. Spantzel, M. Hofrichter, Novel haloperoxidase from the Agaric Basidiomycete *Agrocybe aegerita* oxidizes aryl alcohols and aldehydes, Appl. Environ. Microb. 70 (2004) 4575–4581.
[13] J. Vina-Gonzalez, K. Elbl, X. Ponte, F. Valero, M. Alcalde, Functional expression of aryl-alcohol oxidase in *Saccharomyces cerevisiae* and *Pichia pastoris* by directed evolution, Biotechnol. Bioeng. 115 (2018) 1666–1674.
[14] E. Aranda, M. Kinne, M. Kluge, Ullrich R, M. Hofrichter, Conversion of dibenzothiophene by the mushrooms *Agrocybe aegerita* and *Coprinellus radians* and their extracellular peroxygenases, Appl. Microbiol. Biotechnol. 82 (2009) 1057–1066.
[15] E. Aranda, R. Ullrich, M. Hofrichter, Conversion of polycyclic aromatic hydrocarbons, methyl naphthalenes and dibenzofuran by two fungal peroxygenases, Biodegradation 21 (2010) 267–281.
[16] A. Gutiérrez, E.D. Babot, R. Ullrich, M. Hofrichter, A.T. Martínez, J.C.D. Río, Regioselective oxygenation of fatty acids, fatty alcohols and other aliphatic compounds by a basidiomycete heme-thiolate peroxidase, Arch. Biochem. Biophys. 514 (2011) 33–43.
[17] S. Peter, M. Kinne, X. Wang, R. Ullrich, G. Kayser, J.T. Groves, M. Hofrichter, Selective hydroxylation of alkanes by an extracellular fungal peroxygenase, FEBS J. 278 (2011) 3667–3675.
[18] A. Karich, R. Ullrich, K. Scheibner, M. Hofrichter, Fungal unspecific peroxygenases oxidize the majority of organic EPA priority pollutants, Front. Microbiol. 8 (2017) 1463–1478.
[19] C. Aranda, R. Ullrich, J. Kiebist, K. Scheibner, J.C.D. Río, M. Hofrichter, A. T. Martínez, A. Gutiérrez, Selective synthesis of the resveratrol analogue 4,4′-

dihydroxy-trans-stilbene and stilbenoids modification by fungal peroxygenases, Catal. Sci. Technol. 8 (2018) 2394–2401.
[20] M. Municoy, A.G. Benjumea, J. Carro, C. Aranda, D. Linde, C.R. Mínguez, R. Ullrich, M. Hofrichter, V. Guallar, A. Gutiérrez, A.T. Martínez, Fatty-acid oxygenation by fungal peroxygenases: from computational simulations to preparative regio-and stereoselective epoxidation, ACS Catal 10 (2020) 13584–13595.
[21] E.D. Babot, C. Aranda, J.C.D. Río, R. Ullrich, J. Kiebist, K. Scheibner, M. Hofrichter, A.T. Martínez, A. Gutiérrez, Selective oxygenation of ionones and damascones by fungal peroxygenases, J. Agric. Food Chem. 68 (2020) 5375–5383.
[22] E.D. Babot, J.C.D. Río, L. Kalum, A.T. Martínez, A. Gutiérrez, Oxyfunctionalization of aliphatic compounds by a recombinant peroxygenase from *Coprinopsis Cinerea*, Biotechnol. Bioeng. 110 (2013) 2323–2332.
[23] E.D. Babot, J.C.D. Río, L. Kalum, A.T. Martínez, A. Gutiérrez, Regioselective hydroxylation in the production of 25-hydroxyvitamin D by *Coprinopsis cinerea* peroxygenase, ChemCatCham 7 (2015) 283–290.
[24] A.G. Benjumea, G. Marques, O.M.H. Majumdar, J. Kiebist, K. Scheibner, J.C.D. Río, A.T. Martínez, A. Gutiérrez, High epoxidation yields of vegetable oil hydrolyzates and methyl esters by selected fungal peroxygenases, Front. Bioeng. Biotechnol. 8 (2021) 605854–605866.
[25] A. Olmedo, C. Aranda, J.C.D. Río, J. Kiebist, K. Scheibner, A.T. Martínez, A. Gutiérrez, From alkanes to carboxylic acids: terminal oxygenation by a fungal peroxygenase, Angew. Chem. Int. Ed. 26 (2016) 12436–12439.
[26] A. Olmedo, J.C.D. Río, J. Kiebist, R. Ullrich, M. Hofrichter, K. Scheibner, A. T. Martínez, A. Gutiérrez, Fatty acid chain shortening by a fungal peroxygenase, Chem. Eur. J. 23 (2017) 16985–16989.
[27] J. Carro, A.G. Benjumea, E.F. Fueyo, C. Aranda, V. Gualla, A. Gutiérrez, A. T. Martínez, Modulating fatty acid epoxidation *vs* hydroxylation in a fungal peroxygenase, ACS catal 9 (2019) 6234–6242.
[28] S. Steinbrecht, J. Kiebist, R. König, M. Thiessen, K.U. Schmidtke, S. Kammerer, J. H. Küpper, K. Scheibner, Synthesis of Cyclophosphamide Metabolites By a Peroxygenase from *Marasmius rotula* For Toxicological Studies On Human Cancer Cells, 10, AMB Express, 2020, pp. 128–141.
[29] C. Aranda, A. Olmedo, J. Kiebist, K. Scheibner, J.C.D. Río, A.T. Martínez, Ana Gutiérrez, Selective epoxidation of fatty acids and fatty acid methyl esters by fungal peroxygenases, ChemCatChem 10 (2018) 3964–3968.
[30] J. Kiebist, K.U. Schmidtke, J. Zimmermann, H. Kellner, N. Jehmlich, R. Ullrich, D. Zänder, M. Hofrichter, K. Scheibner, A peroxygenase from *Chaetomium globosum* catalyzes the selective oxygenation of Testosterone, ChemBioChem 18 (2017) 563–569.
[31] C. Aranda, M. Municoy, V. Guallar, J. Kiebist, K. Scheibner, R. Ullrich, J.C.D. Río, M. Hofrichter, A.T. Martínez, A. Gutiérrez, Selective synthesis of 4-hydroxyisophorone and 4-ketoisophorone by fungal peroxygenases, Catal. Sci.Technol. 9 (2019) 1398–1405.
[32] A.G. Benjumea, J. Carro, C.R. Mínguez, D. Linde, E.F. Fueyo, A. Gutiérrez, A. T. Martínez, Fatty acid epoxidation by *Collariella virescens* peroxygenase and heme-channel variants, Catal. Sci. Technol. 10 (2020) 717–725.
[33] L. Rotilio, A. Swoboda, K. Ebner, C. Rinnofner, A. Glieder, W. Kroutil, A. Mattevi, Structural and biochemical studies enlighten the unspecific peroxygenase from *Hypoxylon sp.* EC38 as an efficient oxidative biocatalyst, ACS Catal. 11 (2021) 11511–11525.
[34] A. Knorrscheidt, J. Soler, N. Hünecke, P. Püllmann, M.G. Borràs, M.J. Weissenborn, Accessing chemo- and regioselective benzylic and aromatic oxidations by protein engineering of an unspecific peroxygenase, ACS Catal. 11 (2021) 7327–7338.
[35] M. Faiza, D.M. Lan, S.F. Huang, Y.H. Wang, UPObase: an online database of unspecific Peroxygenases, Database Oxford 2019 (2021) 1–15.
[36] R. Xavier, G Patrice, Deciphering key features in protein structures with the new ENDscript server, Nucleic Acids Res. 42 (2014) 320–324.
[37] Y.J. Ma, H.J. Liang, Z.X. Zhao, B. Wu, D.M. Lan, F. Hollmann, Y.H. Wang, A novel unspecific peroxygenase from *Galatian marginata* for biocatalytic oxyfunctionalization reactions, Mol. Catal. 531 (2022), 112707.
[38] K. Piontek, E. Strittmatter, R. Ullrich, G. Gröbe, M.J. Pecyna, M. Kluge, K. Scheibner, M. Hofrichter, D.A. Plattner, Structural basis of substrate conversion in a new aromatic peroxygenase cytochrome P450 functionality with benefits, JBC 288 (2013) 34767–34776.
[39] Y.J. Ma, Y.R. Li, P.L. Li, W.Y. Zhang, S.J.P. Willot, D. Ribitsch, Y.H. Choi, R. Verpoorte, F. Hollmann, T.Y. Zhang, Y.H. Wang, Natural deep eutectic solvents as multifunctional media for the valorisation of agricultural wastes, ChemSusChem 12 (2019) 1310–1315.
[40] Y.J. Ma, P.L. Li, Y.R. Li, S. Ali, X.Z. Zhang, M.C.R. Rauch, S.J.P. Willot, D. Ribitsch, Y.H. Choi, M. Alcalde, F. Hollmann, Y.H. Wang, Enantioselective sulfoxidation of thioanisole by cascading a choline oxidase and a peroxygenase in the presence of natural deep eutectic solvents, ChemCatChem 12 (2020) 989–994.
[41] Y.J. Ma, Y.R. Li, P.L. Li, X.Z. Zhang, D. Ribitsch, M. Alcalde, Y.H. Wang, F. Hollmann, Natural deep eutectic solvents as performance additives for peroxygenase catalysis, Chempluschem 85 (2020) 254–257.
[42] P.G. dos Santos, et al., Engineering a Highly Regioselective Fungal Peroxygenase for the Synthesis of Hydroxy Fatty Acids, Angew. Chem. 62 (2023), e202217372. Int. Ed.